

Density Functional Theory Studies on the Mechanism of the Reduction of CO₂ to CO Catalyzed by Copper(I) Boryl Complexes

Haitao Zhao,[†] Zhenyang Lin,^{*,†} and Todd B. Marder^{*,‡}

Contribution from the Department of Chemistry and Open Laboratory of Chirotechnology of the Institute of Molecular Technology for Drug Discovery and Synthesis, The Hong Kong University of Science and Technology, Clear Water Bay, Kowloon, Hong Kong, and Department of Chemistry, Durham University, South Road, Durham DH1 3LE, U.K.

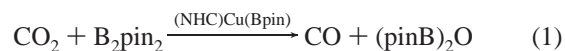
Received May 25, 2006; E-mail: chzlin@ust.hk; todd.marder@durham.ac.uk

Abstract: The detailed reaction mechanism for the reduction of CO₂ to CO catalyzed by (NHC)Cu(boryl) complexes (NHC = *N*-heterocyclic carbene) was studied with the aid of DFT by calculating the relevant intermediates and transition state structures. Our DFT calculations show that the reaction occurs through CO₂ insertion into the Cu–B bond to give a Cu–OC(=O)–boryl species (i.e., containing Cu–O and C–B bonds), and subsequent boryl migration from C to O, followed by σ -bond metathesis between pinB–Bpin (B₂pin₂, pin = pinacolate = OCMe₂CMe₂O) and (NHC)Cu(OBpin). The overall reaction is exergonic by 38.0 kcal/mol. It is the nucleophilicity of the Cu–B bond, a function of the very strong σ -donor properties of the boryl ligand, rather than the oxophilicity of boron, which determines the direction of the CO₂ insertion process. The boryl migration from C to O, which releases the product CO, is the rate-determining step and involves the “vacant” orbital orbital on boron. The (NHC)Cu(boryl) complexes show unique activity in the catalytic process. For the analogous (NHC)Cu(alkyl) complexes, the CO₂ insertion into the Cu–C bond giving a copper acetate intermediate occurs with a readily achievable barrier. However, the elimination of CO from the acetate intermediate through a methyl migration from C to O is energetically inaccessible.

Introduction

Transition metal boryl complexes¹ have attracted considerable interest because of their role in catalyzed hydroboration, diboration, dehydrogenative borylation, and other B–X addition reactions to unsaturated organics,^{2–4} as well as the catalyzed borylation of C–H bonds in alkanes and arenes.⁵ A recent report by Sadighi and co-workers shows that *N*-heterocyclic carbene-ligated copper boryl complexes catalyze oxygen abstraction from CO₂ in solution under mild conditions, that is, the reduction of

CO₂ to CO, with high turnover numbers and frequencies (eq 1).⁶ Reduction of CO₂ to CO is important because CO₂ is naturally very abundant and CO is industrially useful.⁷ It is known that CO₂ can easily insert into an M–E bond (where E = C, H, N, O, P, Si, or other metal),⁸ but it is difficult to break the O=CO bond due to its high bond strength. Why do the copper boryl complexes show such a distinctive catalytic activity in the oxygen abstraction from CO₂? Clearly, there are important implications of this oxygen abstraction for many reactions catalyzed by metal boryl complexes. We decided to study the reaction mechanism in detail. A deep understanding of the reaction mechanism will also lead to more practical systems for the reduction of CO₂.



[†] The Hong Kong University of Science and Technology.

[‡] Durham University.

- (1) For recent reviews, see: (a) Hartwig, J. F.; Waltz, K. M.; Muhoro, C. N.; He, X.; Eisenstein, O.; Bosque, R.; Maseras, F. In *Advances of Boron Chemistry*; Siebert, W., Ed.; Spec. Publ. No. 201; The Royal Society of Chemistry: Cambridge, 1997; p 373. (b) Wadepohl, H. *Angew. Chem., Int. Ed. Engl.* **1997**, *36*, 2441. (c) Irvine, G. J.; Lesley, M. J. G.; Marder, T. B.; Norman, N. C.; Rice, C. R.; Robins, E. G.; Roper, W. R.; Whittell, G. R.; Wright, L. J. *Chem. Rev.* **1998**, *98*, 2685. (d) Braunschweig, H. *Angew. Chem., Int. Ed.* **1998**, *37*, 1786. (e) Smith, M. R., III. *Prog. Inorg. Chem.* **1999**, *48*, 505. (f) Braunschweig, H.; Colling, M. *Coord. Chem. Rev.* **2001**, *223*, 1. (g) Aldridge, S.; Coombs, D. L. *Coord. Chem. Rev.* **2004**, *248*, 535. (h) Braunschweig, H.; Kollmann, C.; Rais, D. *Angew. Chem., Int. Ed.* **2006**, *45*, 5254. For recent structural and computational studies, see, for example: (i) Lam, W. H.; Shimada, S.; Batsanov, A. S.; Lin, Z. Y.; Marder, T. B.; Cowan, J. A.; Howard, J. A. K.; Mason, S. A.; McIntyre, G. J. *Organometallics* **2003**, *22*, 4557. (j) Zhu, J.; Lin, Z.; Marder, T. B. *Inorg. Chem.* **2005**, *44*, 9384.
- (2) (a) Manning, D.; Nöth, H. *Angew. Chem., Int. Ed. Engl.* **1985**, *24*, 878. For reviews, see: (b) Burgess, K.; Ohlmeyer, M. J. *Chem. Rev.* **1991**, *91*, 1179. (c) Burgess, K.; van der Donk, W. A. In *Encyclopedia of Inorganic Chemistry*; King, R. B., Ed.; Wiley: Chichester, 1994; Vol. 3, p 1420. (d) Fu, G. C.; Evans, D. A.; Muci, A. R. In *Advances in Catalytic Processes*; Doyle, M. P., Ed.; JAI: Greenwich, CT, 1995; p 95. (e) Beletskaya, I.; Pelter, A. *Tetrahedron* **1997**, *53*, 4957. (f) Crudden, C. M.; Edwards, D. *Eur. J. Org. Chem.* **2003**, 4695.

- (3) For recent reviews, see: (a) Marder, T. B.; Norman, N. C. *Top. Catal.* **1998**, *5*, 63. (b) Ishiyama, T.; Miyaura, N. *J. Synth. Org. Chem. Jpn.* **1999**, *57*, 503. (c) Ishiyama, T.; Miyaura, N. *J. Organomet. Chem.* **2000**, *611*, 392. (d) Ishiyama, T.; Miyaura, N. *Chem. Rec.* **2004**, *3*, 271. (e) For a recent experimental study on insertion of an alkene into a Cu–B bond, see: Laitar, D. S.; Tsui, E. Y.; Sadighi, J. P. *Organometallics* **2006**, *25*, 2405.
- (4) (a) Musaev, D. G.; Mebel, A. M.; Morokuma, K. *J. Am. Chem. Soc.* **1994**, *116*, 10693. (b) Dorigo, A. E.; Schleyer, P. von R. *Angew. Chem., Int. Ed. Engl.* **1995**, *34*, 115. (c) Widauer, C.; Grützmacher, H.; Ziegler, T. *Organometallics* **2000**, *19*, 2097. For a review, see: (d) Huang, X.; Lin, Z. Y. In *Computational Modeling of Homogeneous Catalysis*; Maseras, F., Lledós, A., Eds.; Kluwer Academic Publishers: Amsterdam, 2002; pp 189–212.

Computational Details

Molecular geometries of the model complexes were optimized without constraints via DFT calculations using the Becke3LYP (B3LYP)⁹ functional. Frequency calculations at the same level of theory have also been performed to identify all of the stationary points as minima (zero imaginary frequencies) or transition states (one imaginary frequency), and to provide free energies at 298.15 K, which include entropic contributions by taking into account the vibrational, rotational, and translational motions of the species under consideration. Transition states were located using the Berny algorithm. Intrinsic reaction coordinates (IRC)¹⁰ were calculated for the transition states to confirm that such structures indeed connect two relevant minima. The 6-311G* Pople basis set¹¹ was used for B and atoms in the CO₂ moiety, while the 6-311G* Wachters–Hay basis set^{12,13} was used for Cu. The 6-31G basis set was used for all other atoms. To examine the basis set dependence, we also employed a larger basis set, 6-311G* for Cu, B, and atoms in the CO₂ moiety and 6-31G* for all other atoms, to carry out single-point energy calculations for several selected structures. The additional calculations show that the basis set dependence is small. For example, using the smaller basis set, the relative energies of **TS**_{Bpin(2–3)}, **4Bpin**, **TS**_{Bpin(4–5)}, **5Bpin**, **6Bpin**, and **TS**_{Bpin(6–1)} (Figure 1a) are 6.7, –23.7, –1.3, –31.4, –43.6, and –31.7 kcal/mol, respectively. Using the larger basis set, the relative energies are 5.9, –24.9, –2.1, –32.6, –43.7, and –32.6 kcal/mol, respectively. Partial atomic charges were calculated on the basis of natural bond orbital (NBO) analyses.¹⁴ All calculations were performed with the Gaussian 03¹⁵ software package.

Results and Discussion

The careful experiments carried out by Sadighi and co-workers allowed them to formulate the catalytic cycle shown in Scheme 1.⁶ In this paper, we examine the detailed reaction mechanism via DFT calculations and show evidence for an unexpected mechanism of insertion. The model catalyst [(NHC)-Cu{B(OR)₂}] {NHC = 1,3-dimethylimidazol-2-ylidene; (OR)₂ = OCH₂CH₂O} was used, in which the substituents at N in the NHC carbene ligand and the methyl groups in the Bpin ligand were replaced by CH₃ and H, respectively. Thus, 1,3-dimethylimidazol-2-ylidene was used to model 1,3-dicyclohexylimidazol-2-ylidene (ICy), while B₂(OCH₂CH₂O)₂ was used to model B₂pin₂.

Based on our DFT calculations, the catalytic cycle shown in Scheme 2 was found to be the most favorable. Figure 1a shows the relevant energy profile. In Figure 1 and the following figures that contain potential energy profiles, calculated relative free energies (kcal/mol) and relative electronic energies (kcal/mol, in parentheses) are presented. The relative free energies and relative electronic energies are similar in cases where the number of reactant and product molecules is equal, for example, one-to-one or two-to-two transformations, but differ significantly for one-to-two or two-to-one transformations because of the entropic contribution. In this paper, relative free energies are used to analyze the reaction mechanism. Figure 2 shows the optimized structures with selected structural parameters for the species involved in this catalytic cycle. In Figure 2, the calculated structures of the model compounds **1Bpin** and **5Bpin** are compared to their corresponding experimental ones.⁶ The calculated geometries reproduce well the important structural parameters. The first step is the CO₂ coordination to the copper center forming a metal- η^2 -carbonyl intermediate **2Bpin**. From **2Bpin**, the coordinated CO₂ then inserts into the M–B bond to give **3Bpin** with a barrier of 3.8 kcal/mol. The small barrier suggests that CO₂ coordination activates the O=CO bond significantly. The step **1Bpin** → **3Bpin** is exergonic by 5.7 kcal/mol, and the overall barrier is 16.0 kcal/mol. Intermediate **3Bpin** then isomerizes to the more stable intermediate, **4Bpin**, with a very small barrier of 2.4 kcal/mol, through a simple rotation of the C(O)Bpin group around the C–O single bond.¹⁶ A CO molecule is released from **4Bpin** with a barrier of 22.0 kcal/mol via a boryl migration from the carbonyl carbon to the metal-bonded oxygen giving **5Bpin**. Coordination of a pinB–Bpin molecule to **5Bpin** gives **6Bpin**. Through a σ -bond metathesis-like transition state, **TS**_{Bpin(6–1)}, the catalyst **1Bpin** is regenerated and pinB–O–Bpin is formed from intermediate **6Bpin** with a barrier of 14.3 kcal/mol. The overall reaction is exergonic by 38.0 kcal/mol, and the conversion of **4Bpin** to **5Bpin** is the rate-determining step. The DFT results thus show that the Cu-catalyzed reduction of CO₂ to CO occurs through CO₂ insertion into Cu–B forming a Cu–O–C–B linkage, and boryl migration from C to O, followed by a σ -bond metathesis between pinB–Bpin and (NHC)Cu(OBpin). The boryl migration, which releases the product CO, is the rate-determining step.

- (5) (a) Iverson, C. N.; Smith, M. R., III. *J. Am. Chem. Soc.* **1999**, *121*, 7696. (b) Waltz, K. M.; Hartwig, J. F. *J. Am. Chem. Soc.* **2000**, *122*, 11358. (c) Chen, H.; Schlecht, S.; Semple, T. C.; Hartwig, J. F. *Science* **2000**, *287*, 1995. (d) Cho, J.-Y.; Iverson, C. N.; Smith, M. R., III. *J. Am. Chem. Soc.* **2000**, *122*, 12868. (e) Tse, M. K.; Cho, J.-Y.; Smith, M. R., III. *Org. Lett.* **2001**, *3*, 2831. (f) Ishiyama, T.; Ishida, K.; Takagi, J.; Miyaura, N. *Chem. Lett.* **2001**, 1082. (g) Shimada, S.; Batsanov, A. S.; Howard, J. A. K.; Marder, T. B. *Angew. Chem., Int. Ed.* **2001**, *40*, 2168. (h) Cho, J.-Y.; Tse, M. K.; Holmes, D.; Maleczka, R. E., Jr.; Smith, M. R., III. *Science* **2002**, *295*, 305. (i) Ishiyama, T.; Tagaki, J.; Ishida, K.; Miyaura, N.; Anastasi, N. R.; Hartwig, J. F. *J. Am. Chem. Soc.* **2002**, *124*, 390. (j) Kondo, Y.; Garica-Cuadrado, D.; Hartwig, J. F.; Boen, N. K.; Wagner, N. L.; Hillmyer, M. A. *J. Am. Chem. Soc.* **2002**, *124*, 1164. (k) Takagi, J.; Sato, K.; Hartwig, J. F.; Ishiyama, T.; Miyaura, N. *Tetrahedron Lett.* **2002**, *43*, 5649. (l) Ishiyama, T.; Takagi, J.; Hartwig, J. F.; Miyaura, N. *Angew. Chem., Int. Ed.* **2002**, *41*, 3056. (m) Wan, X.; Wang, X.; Luo, Y.; Takami, S.; Kubo, M.; Miyamoto, A. *Organometallics* **2002**, *21*, 3703. (n) Webster, C. E.; Fan, Y.; Hall, M. B.; Kunz, D.; Hartwig, J. F. *J. Am. Chem. Soc.* **2003**, *125*, 858. (o) Lam, W. H.; Lin, Z. Y. *Organometallics* **2003**, *22*, 473. (p) Tamura, H.; Yamazaki, H.; Sato, H.; Sakaki, S. *J. Am. Chem. Soc.* **2003**, *125*, 16114. (q) Ishiyama, T.; Miyaura, N. *J. Organomet. Chem.* **2003**, *680*, 3. (r) Kurotobi, K.; Miyauchi, M.; Takakura, K.; Murafuji, T.; Sugihara, Y. *Eur. J. Org. Chem.* **2003**, 3663. (s) Ishiyama, T.; Nobuta, Y.; Hartwig, J. F.; Miyaura, N. *Chem. Commun.* **2003**, 2924. (t) Ishiyama, T.; Takagi, J.; Yonekawa, Y.; Hartwig, J. F.; Miyaura, N. *Adv. Synth. Catal.* **2003**, *345*, 1003. (u) Datta, A.; Köllhofer, A.; Plenio, H. *Chem. Commun.* **2004**, 1508. (v) Lam, W. H.; Lam, K. C.; Lin, Z.; Shimada, S.; Perutz, R. N.; Marder, T. B. *Dalton Trans.* **2004**, 1556. (w) Ishiyama, T. *J. Synth. Org. Chem. Jpn.* **2005**, *63*, 440. (x) Hartwig, J. F.; Cook, K. S.; Hapke, M.; Incarvito, C. D.; Fan, Y. B.; Webster, C. E.; Hall, M. B. *J. Am. Chem. Soc.* **2005**, *127*, 2538. (y) Coventry, D. N.; Batsanov, A. S.; Goeta, A. E.; Howard, J. A. K.; Marder, T. B.; Perutz, R. N. *Chem. Commun.* **2005**, 2172. (z) Chotana, G. A.; Iverson, C. N.; Smith, M. R., III. *J. Am. Chem. Soc.* **2005**, *127*, 10539. (aa) Boller, T. M.; Murphy, J. M.; Hapke, M.; Ishiyama, T.; Miyaura, N.; Hartwig, J. F. *J. Am. Chem. Soc.* **2005**, *127*, 14263. (bb) Mkhaliid, I. A. I.; Coventry, D. N.; Albesa-Jové, D.; Batsanov, A. S.; Howard, J. A. K.; Perutz, R. N.; Marder, T. B. *Angew. Chem., Int. Ed.* **2006**, 489.
- (6) Laitar, D. S.; Müller, P.; Sadighi, J. P. *J. Am. Chem. Soc.* **2005**, *127*, 17196.
- (7) (a) Shibasaki, M.; Yamamoto, Y., Eds. *Multimetallic Catalysts in Organic Synthesis*; Wiley–VCH: Weinheim, Germany, 2004. (b) Ando, H.; Masumura, Y.; Souma, Y. *J. Mol. Catal. A: Chem.* **2000**, *154*, 23.
- (8) (a) Yin, X. L.; Moss, J. R. *Coord. Chem. Rev.* **1999**, *181*, 27. (b) Arakawa, H.; et al. *Chem. Rev.* **2001**, *101*, 953.
- (9) (a) Lee, C. T.; Yang, W. T.; Parr, R. G. *Phys. Rev. B* **1988**, *37*, 785. (b) Becke, A. D. *J. Chem. Phys.* **1993**, *98*, 5648. (c) Miehlich, B.; Savin, A.; Stoll, H.; Preuss, H. *Chem. Phys. Lett.* **1989**, *157*, 200.
- (10) (a) Fukui, K. *J. Phys. Chem.* **1970**, *74*, 4161. (b) Fukui, K. *Acc. Chem. Res.* **1981**, *14*, 363.
- (11) Krishnan, R.; Binkley, J. S.; Seeger, R.; Pople, J. A. *J. Chem. Phys.* **1980**, *72*, 650.
- (12) Wachters, A. J. H. *J. Chem. Phys.* **1970**, *52*, 1033.
- (13) Hay, P. J. *J. Chem. Phys.* **1977**, *66*, 4377.

- (14) (a) Glendening, E. D.; Reed, A. E.; Carpenter, J. E.; Weinhold, F. NBO Version 3.1. (b) Reed, A. E.; Curtiss, L. A.; Weinhold, F. *Chem. Rev.* **1988**, *88*, 849. (c) Foster, J. P.; Weinhold, F. *J. Am. Chem. Soc.* **1980**, *102*, 7211.
- (15) Frisch, M. J.; et al. *Gaussian 03*, revision B.05; Gaussian, Inc.: Pittsburgh, PA, 2003.
- (16) One reviewer suggested that we examine a possible isomer of **4Bpin**, which contains a Cu– η^2 -O₂CBpin bonding mode. Such a structural isomer does not correspond to a local minimum on the potential energy surface.

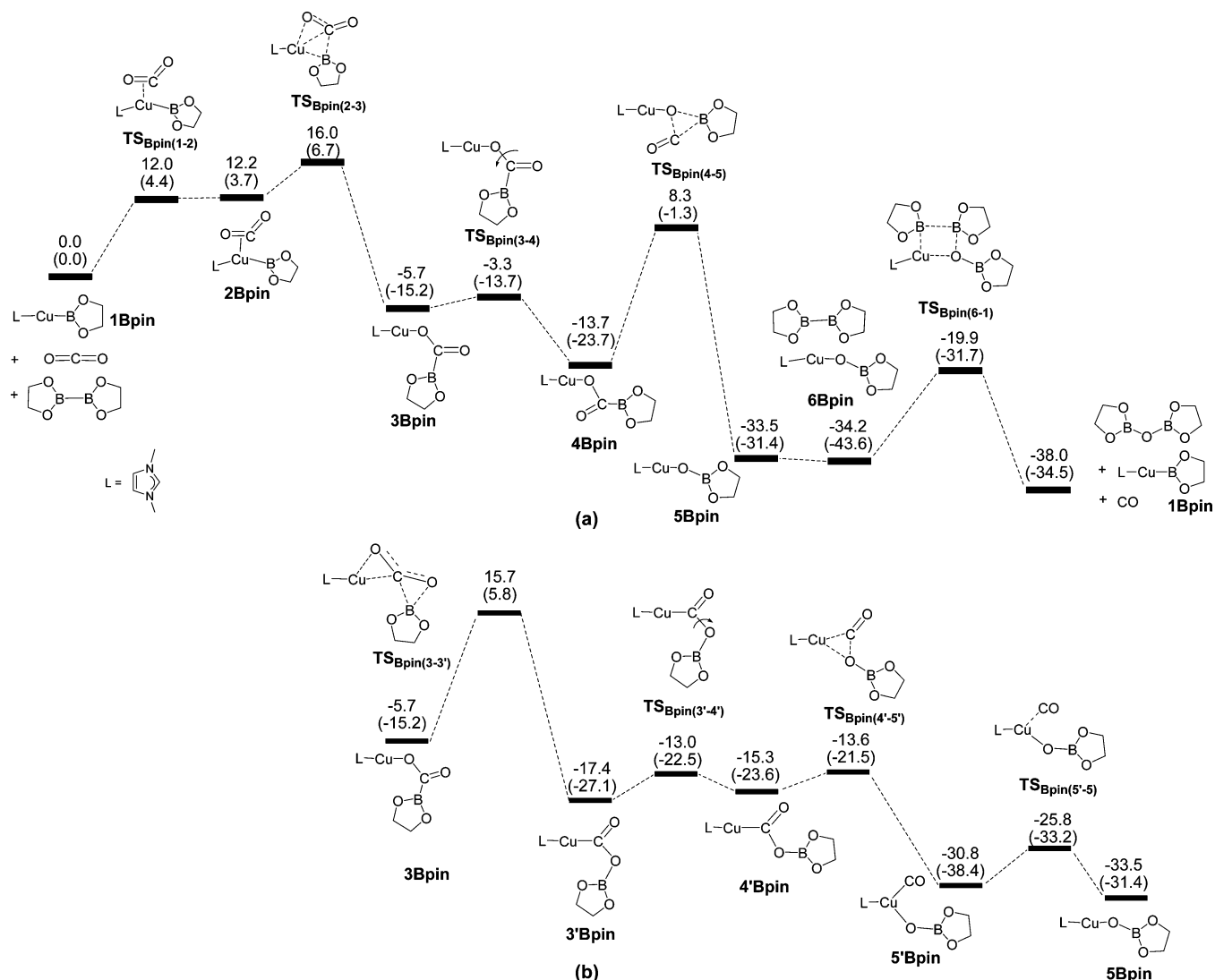
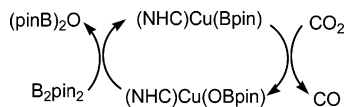
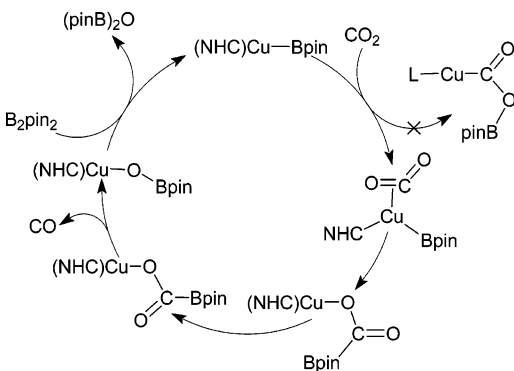


Figure 1. Energy profiles calculated for the (NHC)Cu(boryl)-catalyzed CO₂ reduction to CO: (a) the most favorable reaction pathway and (b) an alternative, but unlikely, reaction pathway. The relative free energies and electronic energies (in parentheses) are given in kcal/mol.

Scheme 1



Scheme 2



The experiments by Sadighi and co-workers show that the reaction turnover frequency is very low when bulkier NHC ligands, such as IPr (IPr = 1,3-bis(2,6-diisopropylphenyl)-imidazol-2-ylidene), are employed.⁶ The bulk of the NHC ligand

can significantly influence the catalyst regeneration step (**6Bpin** → **1Bpin**). Although, on the basis of the model calculations, the catalyst regeneration step is not rate-determining, strong repulsion between a very bulky NHC ligand and B₂pin₂ would increase significantly the energy of the transition state structure, **TS_{Bpin(6-1)}**, making the barrier of the **6Bpin** → **1Bpin** step comparable to that of the rate-determining step. Thus, using the bulky IPr ligand results in low turnover frequencies.

From Figure 1a, we see that the CO₂ insertion step leads to the formation of the Cu–O and C–B bonds in **3Bpin**. When the CO₂ molecule adopts a different orientation in the insertion step, the insertion could give **3'Bpin** with a Cu–C–O–B linkage (Figure 1b), an isomer of **3Bpin**, having Cu–C and O–B bonds. Attempts to locate a metal- η^2 -carbonyl intermediate (**2'Bpin**) similar to **2Bpin** but having a different CO₂ orientation were not successful. Clearly, **2'Bpin** does not correspond to a local minimum. To estimate roughly the energy of **2'Bpin**, we partially optimized a structure in which the Cu–C(CO₂) bond was fixed at 1.999 Å, a distance taken from **2Bpin**. The partially optimized structure is highly unstable and lies 12.9 kcal/mol higher in energy than does **2Bpin**. The assumed **2'Bpin** structure apparently lies even higher in energy

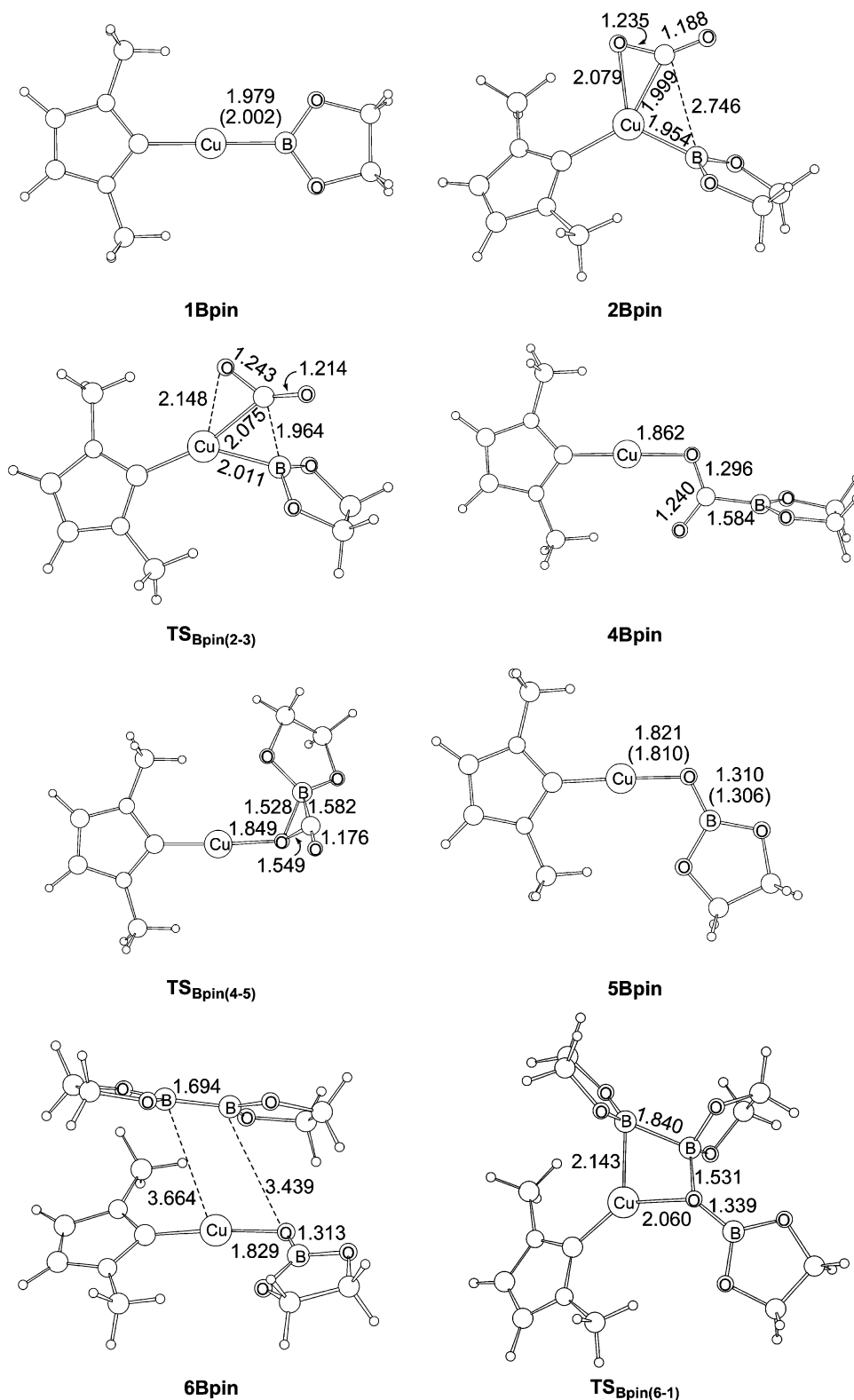


Figure 2. The optimized structures with selected structural parameters (bond length in Å) for the species involved in the most favorable reaction pathway of the (NHC)Cu(boryl)-catalyzed CO₂ reduction. Selected calculated structural parameters for the model compounds **1Bpin** and **5Bpin** are compared to the experimental structural parameters (in parentheses) of (IPr)Cu(Bpin) and (IPr)Cu(OBpin) where IPr = 1,3-bis(2,6-diisopropylphenyl)imidazol-2-ylidene.

than **TS_{Bpin(2-3)}**, the transition state for the CO₂ insertion from **2Bpin**. We can conclude that insertion from the assumed **2'Bpin** is not favored. The B(Bpin)–O(η^2 -O=CO) distance in the calculated **2'Bpin** structure is 3.383 Å (see Figure S1 in the Supporting Information), suggesting a repulsive interaction between the Cu–B bond and the oxygen from the η^2 -

coordinated CO₂ (see below). One might wonder whether insertion giving **3'Bpin** with a Cu–C–O–B linkage would be possible with the bulkier “real” NHC ligand and a B(OCMe₂-CMe₂O) ligand. We do not expect this to be the case. Examining the structures of **2Bpin** and **TS_{Bpin(2-3)}** shown in Figure 2, we do not expect a significant repulsive interaction, between the

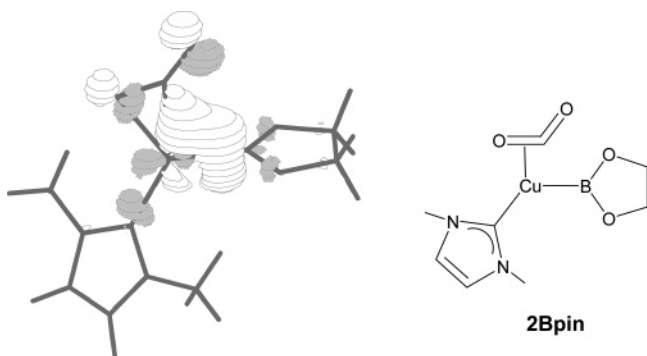


Figure 3. Spatial plots of the HOMO calculated for **2Bpin**.

coordinated CO₂ and the substituents from the NHC and Bpin ligands, which could change our conclusion regarding the CO₂ insertion based on the model ligands.

Examining the bonding characteristics of the HOMO (Figure 3) calculated for **2Bpin**, we found that there exists significant bonding character among the metal center, the boron atom, and the CO₂ carbon. In the HOMO, the back-bonding interaction between the Cu–B σ -bond and the CO₂ carbon can be seen clearly. In other words, the Cu–B σ -bond is involved in a bonding interaction with an empty π^* orbital on the η^2 -CO₂ ligand in **2Bpin**, which is mostly carbon-based. An NBO charge analysis on **2Bpin** shows that there is an electron transfer of $0.53e$ from metal fragment to the CO₂ moiety, suggesting that the back-bonding interaction is significant in **2Bpin**. The absence of such a Cu–B \rightarrow C back-bonding interaction in **2'Bpin** explains the failure to locate it. Attempts to locate a transition state directly connecting **1Bpin** and **3'Bpin** also failed, likely due to the transition state being too high in energy to be found. Interestingly, in contrast to what we see here, in an early study by Morokuma and co-workers,¹⁷ a Cu(I)-to- η^2 -acetylene back-bonding interaction was found to be mainly from a predominantly metal-centered orbital. In **2Bpin**, the Cu–B σ -bonding molecular orbital lies higher in energy than the metal d orbitals, making the Cu–B \rightarrow C back-bonding interaction more important.

To obtain **3'Bpin**, in which the Cu–C and B–O bonds are formed, one might also consider an adduct, which has a B–O Lewis acid–base bond between the boron center of the boryl ligand in the catalyst and one terminal oxygen of CO₂, as a starting species. The calculations show that such an adduct is not a local minimum, suggesting that the Lewis acid–base attraction is very weak. The calculations suggest that the high-energy Cu–B σ -bond, as evidenced by its dominant contribution to the HOMO shown in Figure 3, determines the mode of the CO₂ insertion and that there is no involvement of the “empty” orbital on boron, which interacts strongly with the two oxygens of the pinacolate.

During the attempts to locate the possible transition state structures discussed above, we instead found a new transition state structure connecting **3Bpin** and **3'Bpin** with a barrier of 21.4 kcal/mol from **3Bpin** to **3'Bpin** (Figure 1b). Interestingly, **3'Bpin** easily isomerizes with CO elimination to give **5Bpin** (Figure 1b). Although the **3'Bpin** \rightarrow **5Bpin** conversion is very feasible, the reaction pathway via **3'Bpin** is unlikely because,

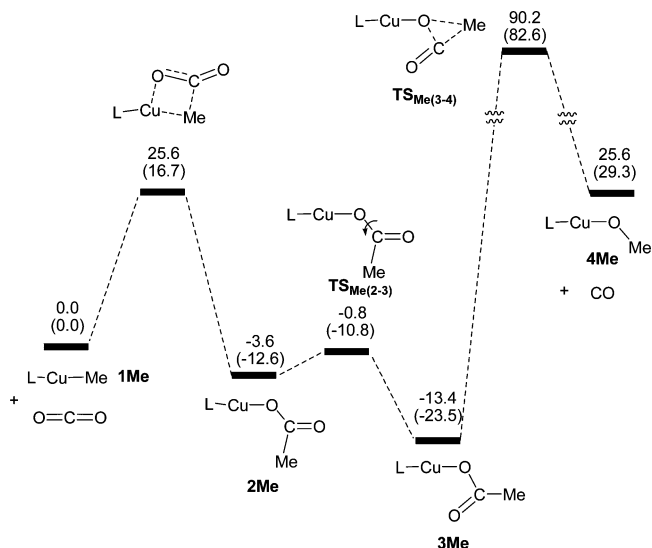


Figure 4. Energy profile for the assumed (NHC)Cu(Me)-catalyzed CO₂ reduction. The relative free energies and electronic energies (in parentheses) are given in kcal/mol.

once formed, **3Bpin** is immediately transformed into **4Bpin** and does not have a chance to undergo the isomerization to **3'Bpin**. One would have to consider a very high overall barrier (29.4 kcal/mol, from **4Bpin** \rightarrow **3Bpin** \rightarrow **TS_{Bpin}(3-3')** \rightarrow **3'Bpin**) if the reaction pathway proceeds via **3'Bpin**.

Experimentally, Sadighi and co-workers also found that CO₂ can insert into the Cu–Me bond of a (IPr)Cu(Me) complex at room temperature to give (IPr)Cu(η^1 -O₂CCH₃).¹⁸ Whereas the predicted (NHC)CuOC(=O)Bpin (**4Bpin**) intermediate extrudes CO very readily, the known (IPr)Cu(η^1 -O₂-CCH₃) has not been observed to do so. We thus examined the difference in reactivities between the Cu–boryl and Cu–alkyl complexes. DFT calculations on the reaction of [(NHC)CuMe] (NHC = 1,3-dimethylimidazol-2-ylidene) with CO₂ were also carried out. Figure 4 shows the energy profile, and Figure 5 shows the optimized structures with selected structural parameters for the species involved. In Figure 5, the calculated structures of the model compounds **1Me** and **3Me** are also compared to their corresponding experimental ones.¹⁸ The optimized structures are again in good agreement with the experimental structures.

Figure 4 shows that the CO₂ insertion into the Cu–C bond of **1Me** gives **2Me** with a barrier of 25.6 kcal/mol (ΔG^\ddagger). Through an isomerization, **3Me**, a model for the insertion product obtained in the experiment,¹⁸ is formed. From Figure 4, we see that **3Me** cannot release CO through a methyl group migration from C to O, due to the very high barrier (103.6 kcal/mol) for such a process. The computational results are consistent with the experimental observation that (NHC)-Cu(Me) does not promote the reduction of CO₂ to CO.

Comparing the energy profiles in Figures 1a and 4, we find that the overall barrier ($\Delta G^\ddagger = 16.0$ kcal/mol) of the CO₂ insertion step in the (NHC)Cu(boryl)-catalyzed CO₂ reduction is smaller than that ($\Delta G^\ddagger = 25.6$ kcal/mol) in the assumed (NHC)Cu(Me)-promoted CO₂ reduction. The insertion barrier is also noticeably smaller than those calculated for the CO₂

(17) Nakamura, E.; Mori, S.; Nakamura, M.; Morokuma, K. *J. Am. Chem. Soc.* **1997**, *119*, 4887.

(18) Mankad, N. P.; Gray, T. G.; Laitar, D. S.; Sadighi, J. P. *Organometallics* **2004**, *23*, 1191.

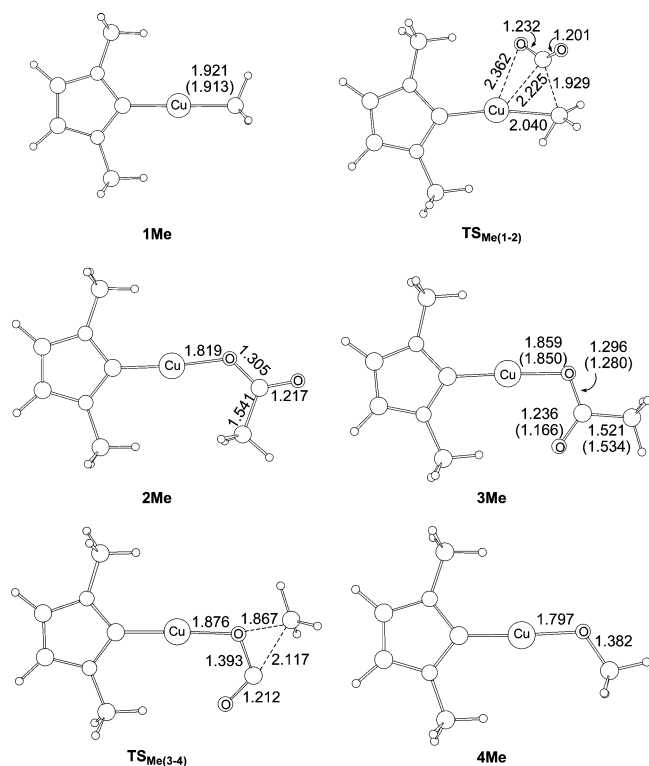


Figure 5. The optimized structures with selected structural parameters (bond length in Å) for the species involved in the assumed (NHC)Cu(Me)-catalyzed CO₂ reduction. Selected calculated structural parameters of the model compounds **1Me** and **3Me** are compared to the experimental structural parameters (in parentheses) of (IPr)Cu(Me) and (IPr)Cu(O₂CCH₃) where IPr = 1,3-bis(2,6-diisopropylphenyl)imidazol-2-ylidene.

insertion into Ru–H and Rh–H bonds.¹⁹ The CO₂ insertion into the Cu–B bond of **1Bpin** proceeds via a CO₂-coordinated intermediate, while the CO₂ insertion into the Cu–C bond of **1Me** proceeds directly without formation of an intermediate. As discussed above, in the CO₂-coordinated intermediate **2Bpin**, the back-bonding interaction between the Cu–B σ -bond and the CO₂ carbon is significant. Therefore, we believe that the greater back-bonding interaction of the Cu–boryl σ -bond versus the Cu–Me σ -bond to the CO₂ carbon explains the smaller barrier found in the CO₂ insertion into the Cu–B bond. The greater back-bonding interaction of the Cu–boryl σ -bond is apparently related to the low electronegativity of boron in the boryl ligand. The lower electronegativity of boron, as compared to carbon, makes the Cu–B σ bond “electron-rich”, in turn increasing the back-donation ability. In other words, the boryl ligand is a much stronger σ -donor than the methyl group, as we found previously.^{1j} To test whether the “electron-richness” argument is justified, we also performed calculations on the insertion of CO₂ in the Cu–B bond of the new model complex (NH₃)Cu(boryl) having NH₃ as the auxiliary ligand, instead of the NHC, as the latter are considered to be strongly trans influencing.²⁰ The CO₂ insertion barrier with this new model complex is ca. 10 kcal/mol greater than that with the (NHC)-Cu(boryl) model complex.

Comparing the boryl and the methyl migrations, both of which would release CO, we found that the former has a much smaller barrier. For the latter, the transition state is energetically inaccessible. In the transition state **TS_{Bpin(4–5)}** for the boryl migration (Figure 2), the boron center in the boryl ligand is tetra-coordinated, suggesting that the “empty” orbital of the boryl ligand assists the migration significantly. The presence of the “empty” orbital avoids exceeding the octet in the transition state of the bond breaking and formation process. In contrast, in the transition state **TS_{Me(3–4)}** for the methyl migration (Figure 5), the carbon center of the migrating methyl group has to adopt a five-coordinate geometry, and, as a result, the C–C and C–O distances are very long. The absence of an “empty” orbital forces the carbon center to exceed the octet, leading to the very long distances calculated for C–C (bond breaking) and C–O (bond forming) in the transition state structure. In the transition state structure **TS_{Me(3–4)}**, the C–C bond is almost broken, while the C–O bond is far from being formed. The barrier (103.6 kcal/mol) calculated for the methyl migration can be considered to be the energy required to break the C–C σ -bond.

Conclusions

The detailed reaction mechanism for the reduction of CO₂ to CO catalyzed by (NHC)Cu(boryl) complexes has been investigated with the aid of DFT calculations. The computational results show that the catalyzed reduction occurs through CO₂ insertion into Cu–B to give a Cu–O–C–B linkage, and boryl migration from C to O, followed by a σ -bond metathesis between pinB–Bpin and (NHC)Cu(OBpin). The boryl migration from C to O, which releases the product, CO, is the rate-determining step.

Our calculations show that the “electron richness” of the Cu–boryl bond, due to the low electronegativity of boron, gives rise to a small CO₂ insertion barrier because the back-bonding interaction between the Cu–B σ -bond and the CO₂ carbon is important in the insertion process. In addition, the NHC auxiliary ligand weakens the Cu–boryl bond due to its strong trans influence. It is the nucleophilicity not the oxophilicity of the Bpin ligand that determines the direction of insertion. We expected that nucleophilicity not oxophilicity is a common feature of many metal–boryl systems for insertion reactions.²¹ We also found that the boryl ligand plays a very important role in the catalytic reactions because it makes the CO elimination possible. The “empty” p-orbital on boron in the boryl ligand allows the boron center to avoid exceeding the octet during the rate-determining boryl migration from C to O, making the CO elimination transition state accessible. In addition, the strength of B–O bonds makes the formation of pinB–O–Bpin from B₂pin₂ a very favorable reaction, providing the thermodynamic driving force for the abstraction of oxygen from CO₂ and other substrates.²²

- (19) (a) Musashi, Y.; Sakaki, S. *J. Am. Chem. Soc.* **2000**, *122*, 3867. (b) Musashi, Y.; Sakaki, S. *J. Am. Chem. Soc.* **2002**, *124*, 7588. (c) Ohnishi, Y.-y.; Matsunaga, T.; Nakao, Y.; Sato, H.; Sakaki, S. *J. Am. Chem. Soc.* **2005**, *127*, 4021.
- (20) Crabtree, R. H. *The Organometallic Chemistry of the Transition Metals*, 4th ed.; John Wiley & Sons, Ltd.: Hoboken, 2005.

- (21) The nucleophilicity feature of a boryl ligand on copper was also found in our preliminary calculations on the diboration of aldehydes catalyzed by (NHC)CuBpin. For the relevant experimental catalytic study, see: Laiter, D. S.; Tsui, E. Y.; Sadighi, J. P. *J. Am. Chem. Soc.* **2006**, *128*, 11036. Nucleophilic copper boryl complexes have been proposed as intermediates in Cu-promoted conjugate addition reactions: Takahashi, K.; Ishiyama, T.; Miyaura, N. *Chem. Lett.* **2000**, 982. Takahashi, K.; Ishiyama, T.; Miyaura, N. *J. Organomet. Chem.* **2001**, *625*, 47. See also: Ito, H.; Yamanaka, H.; Tateiwa, J.; Hosomi, A. *Tetrahedron Lett.* **2000**, *41*, 6821 and, for a very recent example, see: Mun, S.; Lee, J.-E.; Yun, J. *Org. Lett.* **2006**, *8*, 4887. An especially nucleophilic lithium boryl complex has recently been reported: Segawa, Y.; Yamashita, M.; Nozaki, K. *Science* **2006**, *314*, 113. See also: Marder, T. B. *Science* **2006**, *314*, 69.

Acknowledgment. This work was supported by the Research Grant Council of Hong Kong (HKUST 6023/04P and DAG05/06.SC19), the University Grants Committee of Hong Kong through the Area of Excellence Scheme (Aoe/P-10/01). T.B.M. thanks the Royal Society (U.K.) for support via an International

- (22) For the selective deoxygenation of amine oxides, sulfoxides, phosphine oxides, and some organic carbonyl compounds via formation of pinB–O–Bpin, see: (a) Carter, C. A. G.; John, K. D.; Mann, G.; Martin, R. L.; Cameron, T. M.; Baker, R. T.; Bishop, K. L.; Broene, R. D.; Westcott, S. A. *ACS Symp. Ser.* **2002**, 822, 70. (b) Hawkeswood, S.; Stephan, D. W. *Dalton Trans.* **2005**, 2182.

Outgoing Short Visit Grant. We are very grateful to Prof. Joseph Sadighi for helpful discussions and a critical reading of the manuscript.

Supporting Information Available: Tables giving Cartesian coordinates, electronic energies (*E*), free energies (*G*), and zero point energies (ZPE) for all of the calculated structures, and complete refs 8b and 15. This material is available free of charge via the Internet at <http://pubs.acs.org>.

JA063671R